APPARATUS AND DEMONSTRATION NOTES

Jeffrey S. Dunham, *Editor*
Department of Physics, Middlebury College, Middlebury, Vermont 05753

This department welcomes brief communications reporting new demonstrations, laboratory equipment, techniques, or materials of interest to teachers of physics. Notes on new applications of older apparatus, measurements supplementing data supplied by manufacturers, information which, while not new, is not generally known, procurement information, and news about apparatus under development may be suitable for publication in this section. Neither the *American Journal of Physics* nor the Editors assume responsibility for the correctness of the information presented.

A laboratory experiment on internal solitary waves

Daniel Bourgault[a] and Clark Richards[b]
Department of Physics & Physical Oceanography, Memorial University of Newfoundland, St. John's, NL, A1B 3X7, Canada

(Received 30 June 2006; accepted 5 January 2007)

A simple laboratory experiment is designed to show the properties of internal solitary waves. The procedure and analysis are suited for a senior undergraduate laboratory course, though the techniques described may also be used for demonstration purposes in a fluid mechanics course. The measurements collected can be compared to the weakly nonlinear Korteweg–deVries (KdV) theory for the wave shape, lengthscale-amplitude relationship, and phase speed. The experiment provides a good introduction to internal solitary waves in the ocean, along with an exploration of error analysis and the limits of applicability of a theory.
[DOI: 10.1119/1.2437749]

I. INTRODUCTION

Everyone is familiar with ocean waves, the ones that make boats rock and roll. Since the ocean is vertically stratified in temperature and salinity, and thus in density, analogous waves, called *internal waves*, also exist below the sea surface. Although difficult to observe directly, internal waves are thought to be widespread and may play an important role in ocean physics, for transporting and redistributing energy. As their surface counterparts, internal waves may break and enhance turbulent motions that contribute to mixing temperature, salinity, and other constituents such as nutrients and pollutants. However, their origin and propagation properties are not well understood and for that reason they are currently receiving a lot of research attention.[1]

An example of the stratified, or layered, nature of the ocean is illustrated in Fig. 1 from a density profile collected in the Atlantic Ocean. The data show two quasi-homogeneous layers separated by a sharp density gradient, called the pycnocline, at around 32 m depth. This interface, where the density gradient is maximum, can support internal waves. An example of such internal waves is shown in Fig. 2.

Theories exist to describe the properties of internal waves, e.g., phase speed, wavelength, or frequency, given the environmental conditions such as density structure and water depth. The simplest of these, called the linear wave theory,[2] is valid for internal waves that are characterized by very small amplitudes compared to the thickness of the layers between which they propagate. However, oceanic internal waves have frequently been observed to have amplitudes too large to be adequately described by the linear theory.[1] For example, the first wave seen in Fig. 2 has an amplitude of $a \simeq 15$ m compared to the surface layer thickness $h_1 \simeq 10$ m. Under these conditions, that is, when $a/h_1 \sim 1$ or $a/h_2 \sim 1$, the linear wave theory breaks down and other factors, sometimes referred to as *nonlinear effects*, must be taken into account to explain the behavior of such large-amplitude waves.

An important class of nonlinear internal waves are the so-called *internal solitary waves* (ISWs). These waves exhibit the shape of a single hump of unchanging form, as opposed to the sinusoidal shape that characterizes linear waves. For example, a tsunami is a *surface* solitary wave while the first wave seen in Fig. 2 is an internal solitary wave.

We present here a laboratory experiment designed for senior undergraduate physics students, or simply for demonstration purposes, on the existence and propagation of internal solitary waves. This educational experiment is inspired and adapted from existing research experiments.[3,4] The purpose of the experiment is to introduce students to experimental techniques for studying internal waves and to nonlinear wave theory.

II. THEORY

A common simplification to the observed vertical structure of the ocean, useful for theoretical considerations, is the *two-layer model* where the surface and bottom layers are considered homogeneous but of different density and separated by a discontinuity at the pycnocline as shown in Fig. 1. The experiment and the theory we present here are for two-layer fluid systems.

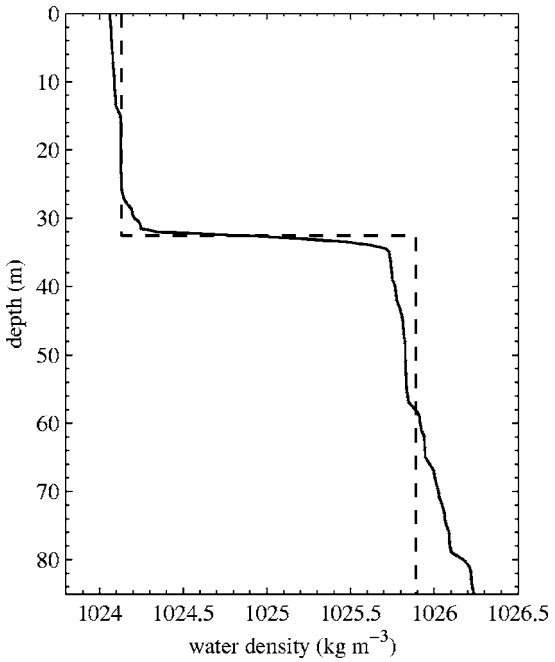

Fig. 1. Density profile observed (solid line) in the Atlantic Ocean off St. John's, Newfoundland, Canada on 29 October 2003 and a two-layer approximation (dashed line).

The characteristics of inviscid weakly nonlinear ISWs, that is, waves with moderate amplitude compared to the layer thicknesses,[4] i.e., for $a/\min(h_1,h_2)\leqslant 0.4$, propagating in a two-layer system of surface and bottom thicknesses h_1 and h_2, respectively, and density difference $\Delta\rho=\rho_2-\rho_1$ are explained by the Korteweg-de-Vries (KdV) theory.[5] This theory predicts that the wave shape is given by

$$\eta(x,t) = a\,\mathrm{sech}^2\left(\frac{x-ct}{\lambda}\right), \tag{1}$$

where η is the interfacial displacement relative to the undisturbed interface and is positive upward; x is the spatial coordinate; t is time; a is the wave amplitude; λ is the wave characteristic lengthscale, also referred to as the half-width; and c is the wave phase speed. A definition sketch is provided in Fig. 3. In theory the wave phase speed, c, is a function of the layer thicknesses, h_1 and h_2, and wave amplitude, a, and is given by

$$c = c_0\left(1+\frac{1}{2}\frac{a|h_1-h_2|}{h_1h_2}\right), \tag{2}$$

where

$$c_0 = \left(g\frac{\Delta\rho}{\rho_2}\frac{h_1h_2}{h_1+h_2}\right)^{1/2} \tag{3}$$

is the phase speed of small-amplitude linear waves. Note that Eq. (2) is valid when $\Delta\rho/\rho_2\ll 1$, which will always be the case for the experiment presented here. The theory further requires that the amplitude a and the half-width λ be related by

$$a\lambda^2 = \frac{4}{3}\frac{(h_1h_2)^2}{(h_1-h_2)}. \tag{4}$$

Note that when the surface layer is thinner than the bottom layer, i.e., $h_1<h_2$, as in the case of Figs. 1 and 2, the right-hand side of Eq. (4) is negative, which means that the amplitude a and therefore the vertical interface displacement η are negative. In this case the ISWs are referred to as waves of depression. In the case where $h_1>h_2$, the amplitude is positive and only waves of elevation are possible, as illustrated in Fig. 3. The intermediate case where $h_1=h_2$ cannot theoretically support ISWs of the KdV type. For practical reasons, the experiment we present here is for waves of elevation, but the theory applies equally well to waves of depression.

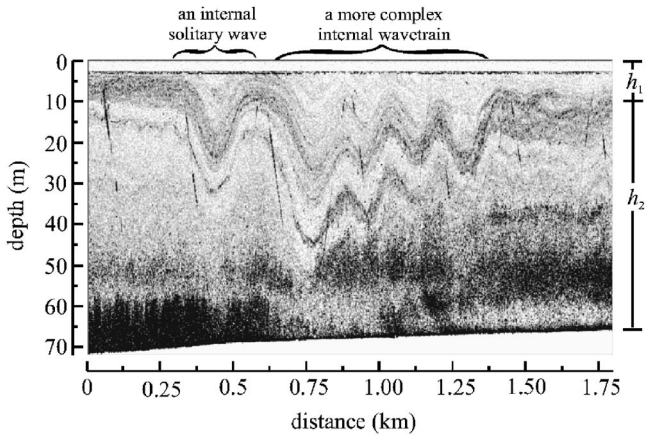

Fig. 2. Leftward-propagating, large amplitude internal wavetrain observed in the St. Lawrence Estuary.[9] The leading wave exhibits the shape of an internal solitary wave of depression and is followed by more complex waves. Here, the surface and bottom layer thicknesses are $h_1\simeq 10$ m and $h_2\simeq 60$ m, respectively. This image was obtained with a ship-based echo-sounder.

III. METHODS

A. General

The experiment is performed in a Plexiglass tank of 100 cm length, 15 cm height, and 10 cm width. Other tank sizes could be used for this experiment. In principle, the longer the tank, the better it is for observing fully developed ISWs that have clearly separated from other types of waves that sometimes arise from our simple generation mechanism. Also, the wider the tank, the better it is for minimizing viscous dissipation arising from sidewall friction. In practice, however, and especially for teaching purposes, the smaller the tank, the easier it is to carry out the experiment because there is less fluid to manipulate. We found our tank size to be convenient and suitable for this educational experiment.

The control parameters are the surface and bottom layer thicknesses h_1 and h_2, respectively, and the density difference $\Delta\rho$ between the layers. It may be left to the students to determine an appropriate range of control parameters to investigate. As an indication of what has worked well for us, our range was $14\text{ cm}\geqslant h_1\geqslant 10\text{ cm}$, $1\text{ cm}\leqslant h_2\leqslant 5\text{ cm}$, $13\text{ kg m}^{-3}\leqslant\Delta\rho\leqslant 44\text{ kg m}^{-3}$.

B. Preparing fluids

Before filling the tank in a two-layer system, as will be explained below, two fluids of different salinity, and thus density, must be prepared for the top and bottom layers. By oceanographic standard, salinity S is a dimensionless quan-

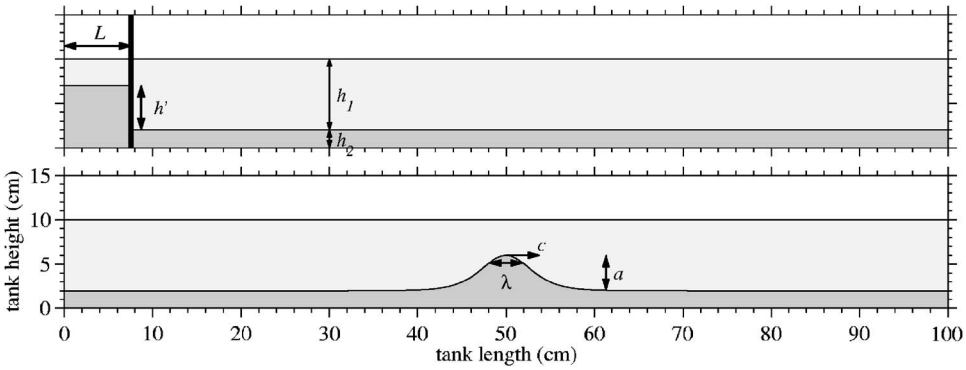

Fig. 3. Definition sketch showing (top) the intial condition used to generate (bottom) an internal solitary wave of elevation of amplitude a, lengthscale λ, and phase speed c, propagating at the interface between the surface layer of thickness h_1 and density ρ_1 (light gray) and the bottom layer of thickness $h_2 < h_1$ and density $\rho_2 > \rho_1$ (darker gray). The thick solid vertical line on the top panel represents a watertight, but easily removable, gate inserted at a distance L from the left end of the tank to create the initial condition. The gate is removed by hand to generate the internal solitary wave.

tity defined as the number of *grams* of salt contained in one *kilogram* of saltwater,[6] that is

$$S \equiv \frac{10^3 M_S}{M_S + M_F}, \tag{5}$$

where M_S is the mass of salt and M_F is the mass of freshwater, both measured in kg. For reference, the average ocean salinity is $S=35$. For this experiment Eq. (5) will be used to determine the mass of salt, M_S, needed to prepare a solution of salinity S given a mass of freshwater, M_F, that is

$$M_S = M_F \frac{S}{10^3 - S}. \tag{6}$$

Note that at room temperature, 21 °C < T < 23 °C, and normal atmospheric pressure, $P=101.3$ kPa, the density of freshwater is $\rho_1 = 9.98 \times 10^2$ kg m^{-3} = 0.998 kg l^{-1}. For all experiments presented here, freshwater, $S_1=0$, is used for the top layer and a salt solution of salinity S_2 is used for the bottom layer. Normal table salt, or pickling salt, which is free of additives, can be used. Once prepared, the salt solution is colored with food dye of any color for visualization.

As explained in Sec. II, what controls internal wave dynamics is not the salinity difference between the layers, but rather the density difference $\Delta\rho = \rho_2 - \rho_1$, as is clear from Eqs. (2) and (3). The densities ρ_1 and ρ_2 can be either measured or calculated. Direct measurements can be obtained if pycnometers or other instruments for measuring water density are available. Otherwise, the density can be calculated conveniently using the linearized equation of state of seawater

$$\rho = \rho_0[1 + \beta(S - S_0)], \tag{7}$$

where $\rho_0 = 1024.76$ kg m^{-3} is a reference density at $T = 20.00$ °C and $S=35.00$, $S_0=35.00$ is a reference salinity, and $\beta = 7.44 \times 10^{-4}$ is the salinity expansion coefficient. The error from using Eq. (7) instead of the full nonlinear equation of state of seawater[7] is small compared to other sources of experimental error.

C. Filling the tank

Filling the tank with the two-layer solution must be done with some care. First, the tank is simply filled with freshwater to the desired upper layer thickness h_1. Second, the colored salt solution is injected slowly underneath the freshwater layer using an apparatus similar to a burette. This is done to minimize mixing between the fluids. For our experiment, we constructed a homemade version using components from a local hardware store, specifically a valve, a length of copper tubing approximately 25 cm long, and a funnel. The tube and the funnel were attached to opposite ends of the valve. The filling device should be clamped in place, with the tube set very close to the bottom of the tank, ~1 mm above the bottom. Once in place, the saltwater can be added into the funnel and the valve opened slightly to allow the saltwater solution to spread slowly underneath the freshwater. The rate of flow can be increased as the bottom layer thickness increases, as long as there is no visible turbulent mixing between the fluids. We keep filling until the saltwater bottom layer reaches the desired thickness h_2. This filling procedure for the tank size used here may take between 15 and 30 min depending on the thickness of the bottom layer h_2 desired.

D. Generating internal solitary waves

Once the tank has been filled, the next step is to create the initial condition necessary for ISW generation. First, a watertight, but removable, gate is inserted all the way to the bottom at a distance L from the left end of the tank, as seen in Fig. 3. Once the gate is in place, saltwater is slowly added to the bottom layer via the burette, until the desired level h', as indicated in Fig. 3, is reached. This should take only a few minutes. Note that there must be a hole in the gate in the surface layer to allow freshwater to flow to the rest of the tank in order to maintain the surface level on both sides of the gate; otherwise surface waves will be generated that will contaminate the experiment. No fluid should be able to leak from one side of the gate to the other in the bottom layer.

As a rule of thumb, the distance L from the left end of the tank to where the gate is inserted could be taken roughly so that the area of added saltwater $A = Lh'$ equals the area displaced by a KdV wave of amplitude $a = h'$, that is $A_{KdV} = \int_{-\infty}^{\infty} \eta(x)\, dx = 2h'\lambda$, with η given by Eq. (1). This tells us that $L \simeq 2\lambda$ and using Eq. (4) we get

$$L \simeq 2\left[\frac{1}{h'}\frac{4}{3}\frac{(h_1h_2)^2}{|h_1-h_2|}\right]^{1/2}. \tag{8}$$

Using a nonideal value of L can cause wavetrains to form behind the leading solitary wave, making analysis more difficult. For a more detailed discussion on wave generation issues, see Ref. 3. For simplicity, the distance L could also be determined by "trial and error."

The wave is set into motion simply by lifting the gate straight out of the tank, allowing the extra volume of saltwater to propagate away from the end. Care must be taken to remove the gate smoothly, so as not to generate excess mixing, and yet quickly, i.e., within about one second, so as to produce a well defined ISW. This procedure may require a few practice runs.

E. Collecting measurements

Analysis of the generated wave is most easily done by recording the motion as a movie using a webcam or a digital camera. Using the recorded digital images of the traveling wave, the phase speed, amplitude, and lengthscale can later be measured in pixel coordinates and scaled to physical units.

The phase speed c is measured by locating the position of the crest of the wave in two consecutive images. Knowing the frame rate of the camera, we can determine the time interval between the frames. The amplitude a is measured relative to the undisturbed interface position, as indicated in Fig. 3. The lengthscale λ can be more difficult to measure unambiguously. Formally, it should be computed as[3]

$$\lambda = \frac{1}{2a}\int_{-\infty}^{\infty} \eta(x)\, dx, \tag{9}$$

where $\eta(x)$ is the vertical displacement relative to the undisturbed interface, which must be digitized from the video images. For an educational experiment, this procedure could be difficult to implement because it depends on the choice of the integration limits, which have to be determined somewhat arbitrarily, since obviously these cannot be taken to be $\pm\infty$. Furthermore, this procedure would require a numerical integration of the digitized interfacial position, which might not be trivial for most undergraduate students to do. Finally, the integration can be contaminated by undesirable disturbances that arise from imperfect initial conditions.

An alternative, somewhat simpler, method is to find the parameters a, λ, x_0, and h that give a best fit of the function

$$\eta_f = a\,\mathrm{sech}^2\left(\frac{x-x_0}{\lambda}\right) + h \tag{10}$$

to the digitized interfacial position η, measured relative to any convenient origin, where η_f is the fitted function. Performing this nonlinear fit requires the students to be proficient with mathematics or data analysis software. Otherwise, the instructor will need to provide source code or teach the students how to perform such a fit, which will be beneficial for them not only for this experiment but for experimental sciences in general. We show in Sec. IV that Eq. (10) gives an acceptable fit to the observed interface even for large-amplitude non-KdV waves, i.e., for waves with $a > 0.4h_2$. Ideally, the fitted parameters above should be supplied with confidence intervals. Many mathematics software packages can provide this. Here we used a bootstrap algorithm[8] to find the 95% confidence intervals on the fitted parameters.

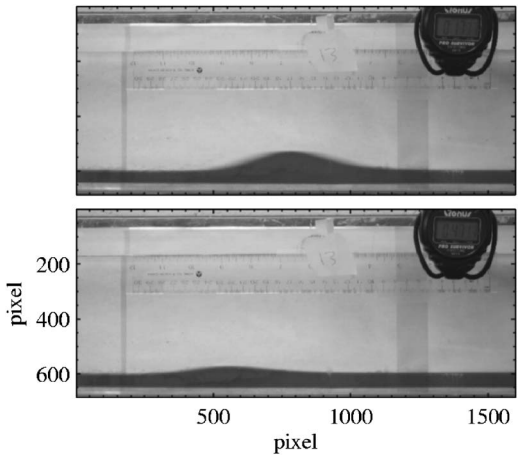

Fig. 4. Examples of an ISW generated in the experiment. The top panel shows the wave during its first passage, propagating rightward. The bottom panel shows the same wave later, after its reflection on the right end of the tank and propagating leftward.

IV. RESULTS

Figure 4 shows a typical example of an ISW generated in one of our experiments with $h_1 = 10.4$ cm, $h_2 = 0.9$ cm, and $\Delta\rho = 43.8$ kg m^{-3}. The top panel of the figure shows the rightward propagating ISW that was generated from our initial condition at the left end of the tank. The bottom panel shows the same wave after its reflection from the right end of the tank, this time propagating leftward. Due to dissipation along the bottom, sidewalls, and across the sheared interface, this reflected wave has a smaller amplitude.

Figure 5 shows the digitized and fitted functions of the waves of Fig. 4. For the larger amplitude wave the fitting gives $a_1 = 1.69 \pm 0.07$ cm and $\lambda_1 = 3.7 \pm 0.2$ cm. For the other wave we obtained $a_2 = 0.49 \pm 0.05$ cm and $\lambda_2 = 3.7 \pm 0.5$ cm. In both cases the fit is significant and the high correlation coefficients, $R \geqslant 0.98$, indicate that Eq. (10) gives an acceptable fit to the measurements, even for large-amplitude waves. Note that the first wave has a normalized amplitude of $a_1/h_2 = 1.7$, indicating a highly nonlinear character, while the second wave, with $a_2/h_2 = 0.5$, has a moderately nonlinear character. The phase speeds for the two waves are $c_1 = 6.6 \pm 0.5$ cm s^{-1} and $c_1 = 6.5 \pm 0.5$ cm s^{-1}, respectively.

It is illuminating for the students to compare the measurements of the half-width-amplitude relationship, $a\lambda^2$, and the

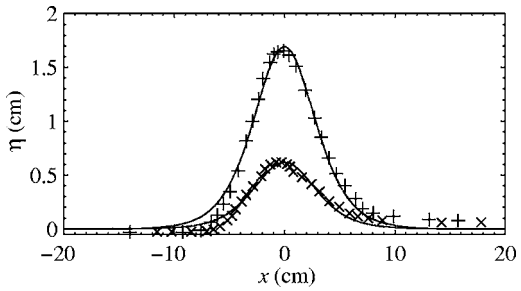

Fig. 5. Digitized, scaled, and centered wave interfacial displacement $\eta(x)$ for the waves shown in Fig. 4. The solid lines are the fit to the measurements.

wave phase-speed, c, to the theoretical predictions of Eqs. (2) and (4). Such a comparison for a number of experiments covering a range of control parameters can be synthesized by graphing the ratio of the measured quantity to its theoretical counterpart, as a function of the ratio a/h_2, similar to Fig. 6 in Ref. 4. Under ideal research laboratory conditions a good fit between the measurements and the theory can be obtained for low amplitude waves,[4] with discrepancies arising for waves with $a/h_2 > 0.4$. Using our simple setup, we found on average that $(a\lambda^2)_{measured}/(a\lambda^2)_{theory} \simeq 1.2$ for ISW characterized with $a/h_2 < 0.4$. Largest ratios reached about $(a\lambda^2)_{measured}/(a\lambda^2)_{theory} \simeq 3$ for large-amplitude ISW characterized with $a/h_2 \sim 1$. For the phase speed we found on average that $c_{measured}/c_{theory} \simeq 0.8$, with no significant dependence on a/h_2. This systematic disagreement between the measured values and the theory for the phase speed is presumably due to friction caused by the bottom and the side of the tank, which is not taken into account in the KdV theory. We thus attribute some of the differences between the theory and the measurements to experimental limitations associated with the simple equipment and techniques used.

V. CONCLUSION

We have described a simple experiment demonstrating the properties of internal solitary waves. The experiment is suitable for demonstration purposes, or potentially for an advanced undergraduate laboratory course. Techniques for creating and analyzing internal waves, as well as some discussion regarding comparison with theory, have been presented. While it is difficult to obtain a good fit between the theory and the measurements, this simple experiment can serve to introduce students to the difficulties of making accurate comparisons between predictions and data.

ACKNOWLEDGMENTS

This work was funded by the Department of Physics & Physical Oceanography, Memorial University of Newfoundland. We are thankful to Dr. C. Deacon (MUN) for technical support and to R. Mirshak and Dr. D. Kelley (Dalhousie University) for their helpful comments on the original manuscript.

[a]Electronic mail: danielb@physics.mun.ca

[b]Present address: Department of Oceanography, Dalhousie University, 1355 Oxford Street, Halifax, NS, B3H 4J1, Canada. Electronic mail: clark.richards@dal.ca

[1] K. R. Helfrich and W. K. Melville, "Long nonlinear internal waves," Annu. Rev. Fluid Mech. **38**, 395–425 (2006).

[2] P. K. Kundu and I. M. Cohen, *Fluid Mechanics* (Academic, San Diego, 2004), p. 240.

[3] T. W. Kao, F.-S. Pan, and D. Renouard, "Internal solitons on the pycnocline: generation, propagation, and shoaling and breaking over a slope," J. Fluid Mech. **169**, 19–53 (1985).

[4] J. Grue, A. Jensen, P.-O. Rusas, and J. K. Sveen, "Properties of large-amplitude internal waves," J. Fluid Mech. **380**, 257–278 (1999).

[5] D. Bogucki and C. Garrett, "A simple model for shear-induced decay of an internal solitary wave," J. Phys. Oceanogr. **23**, 1767–1776 (1993).

[6] S. Pond and G. L. Pickard, *Introductory Dynamical Oceanography*, 2nd ed. (Butterworth-Heinemann, 1983).

[7] A. E. Gill, *Atmosphere-Ocean Dynamics* (Academic, San Diego, CA, 1982), p. 599.

[8] W. Press, S. Teukolsky, W. Vetterling, and B. Flannery, *Numerical Recipes in FORTRAN. Second edition* (Cambridge U. P., New York, 1992), p. 686.

[9] D. Bourgault, F. J. Saucier, and C. A. Lin, "Shear instability in the St. Lawrence Estuary, Canada: A comparison of fine-scale observations and estuarine circulation model results," J. Geophys. Res. **106**, 9393–9409 (2001).